

Status of Silicon Carbide Joining and Irradiation Studies

July 31, 2013

**Y. Katoh
J. O. Kiggans
C. Shih
T. Koyanagi
J. L. McDuffee
L.L. Snead**

DOCUMENT AVAILABILITY

Reports produced after January 1, 1996, are generally available free via the U.S. Department of Energy (DOE) Information Bridge.

Web site <http://www.osti.gov/bridge>

Reports produced before January 1, 1996, may be purchased by members of the public from the following source.

National Technical Information Service
5285 Port Royal Road
Springfield, VA 22161
Telephone 703-605-6000 (1-800-553-6847)
TDD 703-487-4639
Fax 703-605-6900
E-mail info@ntis.gov
Web site <http://www.ntis.gov/support/ordernowabout.htm>

Reports are available to DOE employees, DOE contractors, Energy Technology Data Exchange (ETDE) representatives, and International Nuclear Information System (INIS) representatives from the following source.

Office of Scientific and Technical Information
P.O. Box 62
Oak Ridge, TN 37831
Telephone 865-576-8401
Fax 865-576-5728
E-mail reports@osti.gov
Web site <http://www.osti.gov/contact.html>

This report was prepared as an account of work sponsored by an agency of the United States Government. Neither the United States Government nor any agency thereof, nor any of their employees, makes any warranty, express or implied, or assumes any legal liability or responsibility for the accuracy, completeness, or usefulness of any information, apparatus, product, or process disclosed, or represents that its use would not infringe privately owned rights. Reference herein to any specific commercial product, process, or service by trade name, trademark, manufacturer, or otherwise, does not necessarily constitute or imply its endorsement, recommendation, or favoring by the United States Government or any agency thereof. The views and opinions of authors expressed herein do not necessarily state or reflect those of the United States Government or any agency thereof.

Materials Science and Technology Division

Status of Silicon Carbide Joining and Irradiation Studies

Y. Katoh, J.O. Kiggans, C. Shih, T. Koyanagi, J.L. McDuffee, and L.L. Snead

Materials Science and Technology Division, Oak Ridge National Laboratory

Date Published: July 2013

Prepared for the
United States Department of Energy –
Office of Nuclear Energy
under the
Light Water Reactor Sustainability Program's
Advanced LWR Nuclear Fuels Pathway

CONTENTS

	Page
CONTENTS	iii
LIST OF FIGURES	v
LIST OF TABLES	vii
1. SUMMARY	9
2. SILICON CARBIDE JOINT PREPARATION AND EVALUATION	11
2.1 METHODS OF JOINING	11
2.1.1 Overview	11
2.1.2 Metallic diffusion bonding	11
2.1.3 MAX-phase bonding	11
2.1.4 NITE joining.....	12
2.2 MECHANICAL TESTING AND CHARACTERIZATION	12
2.2.1 Strength evaluation.....	12
2.2.2 Microstructural characterization.....	13
2.3 RESULTS.....	14
2.3.1 Ti diffusion bonding.....	15
2.3.2 Mo diffusion bonding.....	17
2.3.3 MAX-phase pressureless joining.....	18
2.3.4 NITE joining.....	18
3. IRRADIATION PROGRAM	21
3.1 TEST METRIX AND SCHEDULE.....	21
3.2 IRRADIATION VEHICLE DEVELOPMENT	22
4. REFERENCES	23
Appendix A: Capsule design Drawings	25
Appendix B: Specimen Drawings	29
Appendix C: Updated Thermal Analysis Results.....	35

LIST OF FIGURES

	Page
Figure 1 Schematic of the double-notched compression test specimen.	13
Figure 2. Schematic (left) and a photographic image (right) of test fixture for the double-notched compression test specimen.	13
Figure 3. A schematic illustration of Ti joint microstructure evolution at various temperatures.	15
Figure 4. Back Scattering Electron (BSE) image of Ti diffusion-bonded joints.	16
Figure 5. Secondary electron (SE) images of Mo foil joint hot pressed at 1300°C for 1 h: (a) joint interface before DNS test and (b) joint interface after DNS test.	17
Figure 6. Back scattering electron (BSE) images of the Mo joints formed at 1500 and 1700 °C with and without oxygen eliminator.	18
Figure 7. Back scattering electron (BSE) images of NITE slurry joint hot pressed at 1860°C for 1h.	19
Figure 8. Secondary electron images of ultrasonically spray-coated NITE slurry joint hot pressed at 1875°C for 1 h. (a, b): Well sintered region with large pores; (c, d): more porous region.	20

LIST OF TABLES

	Page
Table 1. Status summary of SiC joint processing in the present work.....	11
Table 2. Processing conditions, shear strengths, joint microstructures and fracture behaviors of CVD-silicon carbide joined by different joining materials	14
Table 3. List of capsules and irradiation conditions. The Round A irradiation is currently scheduled to initiate in early FY-2014. The Round B irradiation is temporarily planned to initiate in FY-2015.	21
Table 4. Updated schedule of the irradiation program	22
Table 5. Materials considered for irradiation study.....	22

1. SUMMARY

Development of silicon carbide (SiC) joints that retain adequate mechanical and functional properties in the anticipated service conditions is a critical milestone toward establishment of advanced ceramic composite technology for the light water reactor (LWR) fuels and core structures. Neutron irradiation is among the most critical factors that define the service condition of LWR fuel during the normal operation. The overarching goal of the present joining and irradiation studies is to establish technologies for joining SiC-based materials for use as the LWR fuel cladding. The purpose of this task LW-13OR0504073 is to prepare rabbit capsules and SiC joint specimens for irradiation study in High Flux Isotope Reactor (HFIR). The present report, an update to ORNL/TM-2012/597, summarizes the progress in this task activity through July 2013.

2. SILICON CARBIDE JOINT PREPARATION AND EVALUATION

2.1 METHODS OF JOINING

2.1.1 Overview

Development of the joining technologies and preparation of the joint materials for evaluation, including the effects of neutron irradiation, have been pursued using high purity monolithic SiC as the base material to be joined together. The methods and the development status of the SiC joining studied at Oak Ridge National Laboratory (ORNL) in support of the Light Water Reactor Sustainability (LWRS) Fuels Program are listed in Table 1.

Table 1. Status summary of SiC joint processing in the present work.

Method	Insert Material	Status
Metallic diffusion bonding	Ti foil	Optimum joining condition established
	Mo foil	Optimum joining condition established
MAX-phase bonding	Ti-Si-C slurry	Successful with commercial joining kit
Transient eutectic-phase joining	NITE* slurry	Optimum joining condition being studied

*NITE: Nano-Infiltration and Transient Eutectic-phase process for sintering SiC

2.1.2 Metallic diffusion bonding

Ti foil bonding: Flat, rectangular plates of chemically vapor-deposited (CVD) SiC (Dow Chemical, Marlborough, MA) were joined by hot pressing with an insert of Ti foil (0.025mm thick, 99.94%, Alfa Aesar) at temperatures 1300 or 1500 °C and pressures 15 to 20 MPa for durations 1 to 5 hrs under vacuum.

Mo foil bonding: Flat, rectangular plates of CVD SiC were joined by hot pressing with an insert of Mo foil (0.025mm thick, 99.95%, Alfa Aesar) at temperatures 1300 to 1700 °C and pressure 20 MPa for durations 1 hr under vacuum or Ar atmosphere.

2.1.3 MAX-phase bonding

A set of joining agent materials were purchased from Hyper-Therm High Temperature Composites, Inc. (currently Rolls-Royce High Temperature Composites, Inc., or Rolls-Royce HTC, Huntington Beach, CA) Ti₃SiC₂-based joints of CVD SiC were produced at ORNL based on a pressureless slurry process per instruction by the vender. Details of the raw materials and the process condition are proprietary.

2.1.4 NITE joining

A thin coating layer of NITE formula was applied either by hand-painting of the slurry or by an ultrasonic spraying on a face of CVD SiC specimen placed face to face to form a sandwich. Joining was performed in a hot-press furnace in a flowing Ar atmosphere at temperatures 1860 to 1875 °C and a uniaxial pressure 20 MPa for 1 hr under Ar atmosphere.

2.2 MECHANICAL TESTING AND CHARACTERIZATION

2.2.1 Strength evaluation

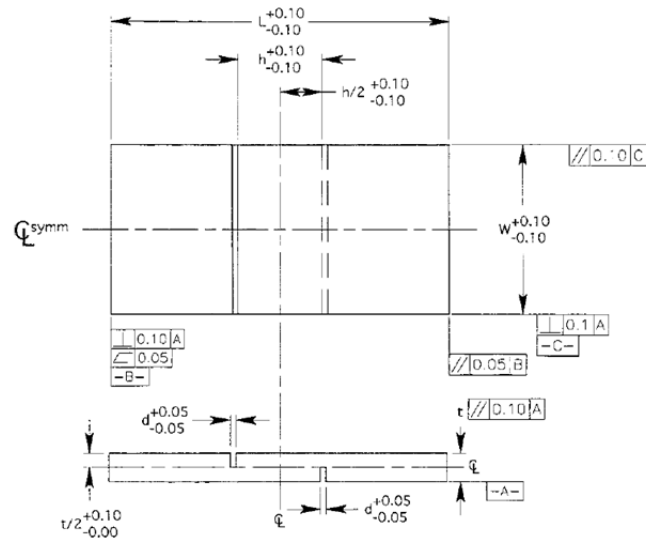
It is the plan that the effect of neutron irradiation on strength of the SiC joints will be determined by torsional shear tests using solid hourglass type specimens. The torsional shear test is near ideal for this purpose because of its ability to apply true shear loading to the joint specimens and simple test procedure.

A new Standard Test Method for Torsional Shear Strength of Bonded Joints of Advanced Ceramics at Ambient Temperature is currently under development in ASTM Subcommittee C28.04 on Ceramic Applications under Committee C28 on Advanced Ceramics. The new test standard will be based on the test development in the present and related programs for studies on silicon carbide joining technologies for nuclear and fusion energy applications. More detailed information of this standard development status and activity is available from the subject work item technical contact, Dr. S.T. Gonczy of Gateway Materials Technology, Inc.

In this work, the joint strength was estimated by loading a double-notched test specimen of uniform width in compression, which is the standard test method ASTM C1292 for inter-laminar shear strength of continuous fiber-reinforced advanced ceramics at ambient temperatures. This test method, often referred to as double-notch shear (DNS) test, is in principle a variation of the offset single lap shear test as defined in ASTM D905 with an improved alignment capability due to the presence of the extended end sections. The DNS shear test is particularly useful for the purpose of quick estimation of developmental joints. The hot-pressed plates were machined into DNS specimens according to the dimension scheme shown in

Figure 1. The actual dimensions adopted were $L = 20$ mm, $W = 6$ mm, $t = 7.6$ mm, $h = 1.3$ mm, and $d = 3$ mm.

Figure 2 shows a schematic and a photograph of the test setup. Failure of the test specimen occurs by shear between two centrally located notches machined halfway through the thickness and spaced a fixed distance apart on opposing faces (ASTM 1292).



NOTE 1—All tolerances are in millimetres.

Figure 1 Schematic of the double-notched compression test specimen.

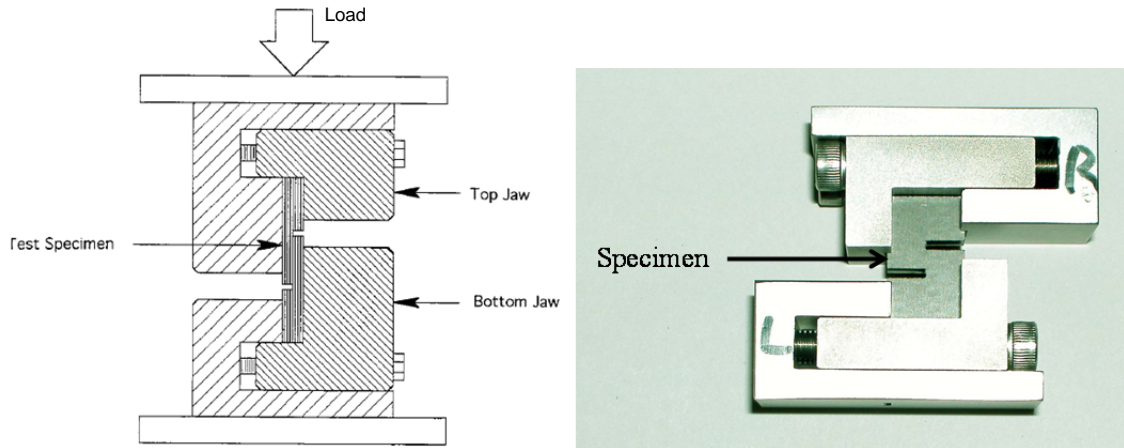


Figure 2. Schematic (left) and a photographic image (right) of test fixture for the double-notched compression test specimen.

2.2.2 Microstructural characterization

Polished cross-sections of the tested specimens were characterized using field-emission-gun scanning electron microscopy (FEG-SEM) in a Hitachi Model S4800, equipped with energy dispersive spectroscopy (EDS). The surface phases formed and their relative amounts were determined by X-ray diffraction (XRD) analysis (Model Scinatag Pad V, Thermo ARL). (NOTE: all SEM images shown below were taken on specimens after shear testing.)

2.3 RESULTS

The processing parameters including hot pressing temperature, pressure, time, and joining material thickness were selected based on thorough literature review. Multiple joining conditions were attempted for each joining material in order to determine their optimal processing conditions which will be used for fabricating the joint specimens for irradiation behavior study. Table 2 lists the selected processing conditions, shear strengths, joint microstructures and fracture behaviors observed in the present study.

Table 2. Processing conditions, shear strengths, joint microstructures and fracture behaviors of CVD-silicon carbide joined by different joining materials

Insert materials	Specimen ID	Temp. (°C)	Press. (MPa)	Time (h)	Shear Strength (MPa)	S.D. (MPa)	Phases	Joint Appearance	Failure Location
Ti foil	Tif-1300-1	1300	20	1	1.7		Ti ₅ Si ₃ , TiC	Ti ₅ Si ₃ /SiC debonding	Interface
	Tif-1500-1	1500	15	1	97.6	8.8	85.1% TiC, Ti ₃ SiC ₂	Intact	Through joint
	Tif-1500-5	1500	20	5	28.4	13.7	Ti ₃ SiC ₂	Intact	Mix
Mo foil	Mof-1300-1	1300	20	1	46.4	30.6	Mo ₂ C, Mo ₅ Si ₃	Porous interface	Interface
	Mof-1300-5	1300	20	5	15.2	7.2	Mo ₂ C, Mo ₅ Si ₃	Intact	Interface and base
	Mof-1500-1	1500	15	1	55.2	15.4	Mo ₂ C, Mo ₅ Si ₃	Intact	Through joint
	Mof-1500-1-Ti ¹	1500	15	1	83.1	41.7	Mo ₂ C, Mo ₅ Si ₃	Intact	Mostly base
	Mof-1500-1-H ₂ ²	1500	15	1	105.5	4.6	Mo ₂ C, Mo ₅ Si ₃	Intact	Base
	Mof-1500-5	1500	20	5	18.8	11.2	Mo ₂ C, Mo ₅ Si ₃	Partially debonding	Primarily at base
	Mof-1700-1	1700	20	1	68.2	18.7	Mo ₂ C, Mo ₅ Si ₃	Intact	Mostly base
	Mof-1700-1-H ₂ ²	1700	20	1	94	20.6	Mo ₂ C, Mo ₅ Si ₃	Intact	Mostly base
HHTC MAX	HMX	N/D ³	N/D	N/D	69.9	6.3	N/D	Intact	Interface
NITE slurry	NITEs-1860-1	1860	20	1	43.9	38.8	SiC	Porous/dense joint, debonding at porous joint	Interface at porous joint
NITE spray	NITEc-1875-1	1875	20	1	67.3	33.2	SiC	Porous/dense joint, debonding at porous joint	Interface at porous joint

1, 2: Suffix Ti indicates that titanium powder was used as an oxygen getter in vacuum environment. Suffix H₂ indicates that hydrogen was added to flowing argon atmosphere. Other processing runs were performed in vacuum for metal diffusion bonding. NITE processing runs were performed in an argon flow.

3: not disclosed

2.3.1 Ti diffusion bonding

For Ti diffusion bonding, a scheme representing the Ti joint microstructure evolution at different hot-pressing temperatures was developed by Gottselig [1], shown in

Figure 3. Low temperature ($<1250^{\circ}\text{C}$) may result into complex interlayer structures, which may not be favorable in robust process design and mechanical property control. Therefore, temperatures in a range of $1300\text{-}1500^{\circ}\text{C}$ were selected for Ti joining in this work.

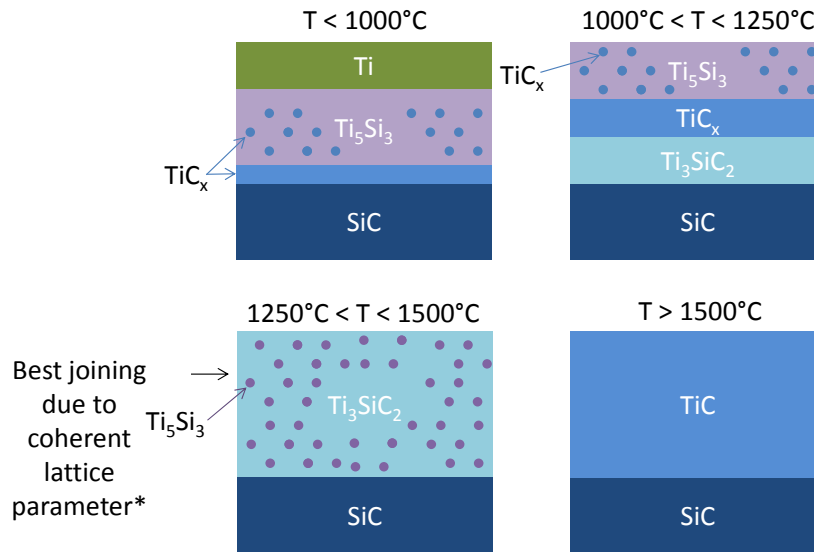


Figure 3. A schematic illustration of Ti joint microstructure evolution at various temperatures.

Pressure higher than 10 MPa has no effect on bonding quality [1, 2]. Therefore, slight variance in pressure, e.g. 15MPa and 20 MPa shall not result into obvious joint microstructure evolution. Temperature and time effects are examined in this work. Figure 4 (a) shows the microstructure of the Ti joint formed after hot pressing at 1500°C for 1h. The Ti foil was completely reacted with SiC by forming TiC (primary product) and Ti_3SiC_2 , evidenced by XRD spectrum (not shown here) in which no Ti metal phase was detected. In Figure 4 (b), the Ti joint seems homogenous and no phase contrast was observed, suggesting that the fine Ti_3SiC_2 grains may disperse in the TiC matrix. Cracks were found in the joint, indicating its brittle character. The formed TiC phase has good wetting behavior on SiC, evidenced from good contact at the joint/substrate interface. Time effect was analyzed by extending hot pressing time to 5 hrs but keeping the temperature and pressure constant, and the microstructure of the formed Ti joint was illustrated in Figure 4 (c). A uniform Ti_3SiC_2 interlayer was formed under the above conditions, indicating that Si diffusion dominated in extensive time by reacting with TiC, forming Ti_3SiC_2 . No interfacial debonding was observed. Hot pressing at a lower temperature of 1300°C was also performed to examine the temperature effect. The microstructure of Ti joint formed at 1300°C for 1 h is shown in Fig. 6. The TiC phases (dark) with small and large grains are dispersed in Ti_5Si_3 (bright) matrix which is adjacent to SiC base. Interfacial debonding is clearly observed in Figure 4 (c), possibly due to large coefficient of thermal expansion (CTE) mismatch between SiC and Ti_5Si_3 . Those results suggest that the Ti foil joining prefers high temperature, e.g. 1500°C , in order to

achieve good interfacial bond with the SiC base.

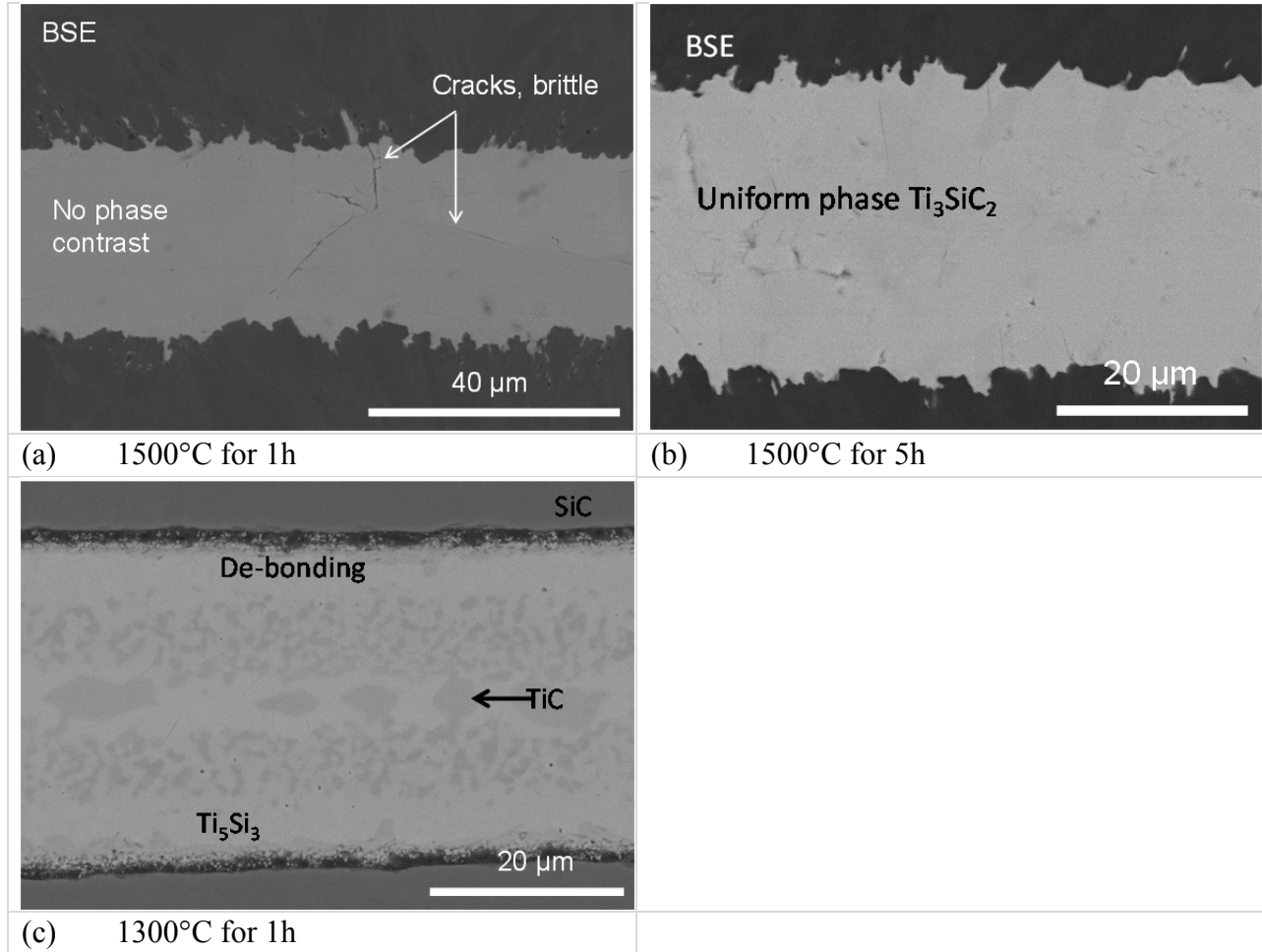


Figure 4. Back Scattering Electron (BSE) image of Ti diffusion-bonded joints.

The Ti joint strengths of the specimens hot pressed under different conditions are listed in Table 2. The joints formed after hot pressing at 1500°C for 1 h show the highest shear strength of 98 MPa and a small standard deviation of 9MPa. In contrast, the joints formed at 1300°C for 1 h shows the lowest strength, some of which were actually broken during machining. Those strength results are consistent with the microstructures presented above, showing good interfacial contact at 1500°C and interfacial de-bonding at 1300°C, respectively. The low strength provided by Ti joint hot pressed at 1500°C for 5 h was surprising, because the formed uniform Ti_3SiC_2 phase was expected to show good strength due to the good CTE match with SiC. Certain amount of oxygen was detected in such joint using SEM-EDS, but absence in the Ti joint formed in 1h hot pressing. Oxygen embedment during extensive reaction may lead to the unexpected low joint strength. Based on the present observation, a measure of oxygen removal will be taken for production of future joint materials including those for the neutron irradiation study. The Ti joint hot pressed at 1500°C for 1 h exhibits the desired strength, therefore, its processing conditions

have been chosen for fabricating the Ti joined CVD-SiC specimens for future irradiation tests.

2.3.2 Mo diffusion bonding

Previously reported results [3] indicated: (1) short-time (1 h) hot pressing is sufficient to obtain good quality joints; (2) Mo foil is favored over Mo powder slurry as the joining material because it experiences much less volume shrinkage during hot pressing; and (3) oxygen is suspected to have caused low strength in certain joining condition because a detectable amount of oxygen was observed in the Energy Dispersive X-ray spectrum of the joint. Therefore, an oxygen getter (e.g. Ti) and hydrogen gas have been used in the following Mo foil joining processes, performed at temperatures of 1300, 1500, and 1700°C and pressures of 20 MPa for 1 h. Compared with other Mo joints, the one formed at 1500°C for 1 h in a H₂/Ar gas flow exhibits the maximum strength of 106 MPa and the minimum standard deviation of 4.6 MPa. In contrast, the Mo joint formed in vacuum shows a significantly lower strength of 55 MPa. Using Ti powder to absorb O₂ also improves the Mo joint strength to a moderate extent. However, Ti powder tends to aggregate due to sintering at high temperatures, gradually losing its reactivity during hot pressing, which is also the reason of using H₂ instead of Ti at 1700°C. As expected, applying H₂ gas increases strength of the Mo joint formed at 1700 °C from 68 to 94 MPa on average, as shown in Table 2.

The low strength of the Mo joint produced at 1300°C for 1 h is likely caused by the large number of pores along the joint interface, Figure 5 (a), because the fracture location was mainly at joint/base interface as shown in Figure 5 (b). The Mo₅Si₃ phase was formed adjacent to the Mo foil/SiC interface. While some Si was detected in the middle of the joint due to atom diffusion, extensive amount of Mo foil still remains intact in this joining condition.

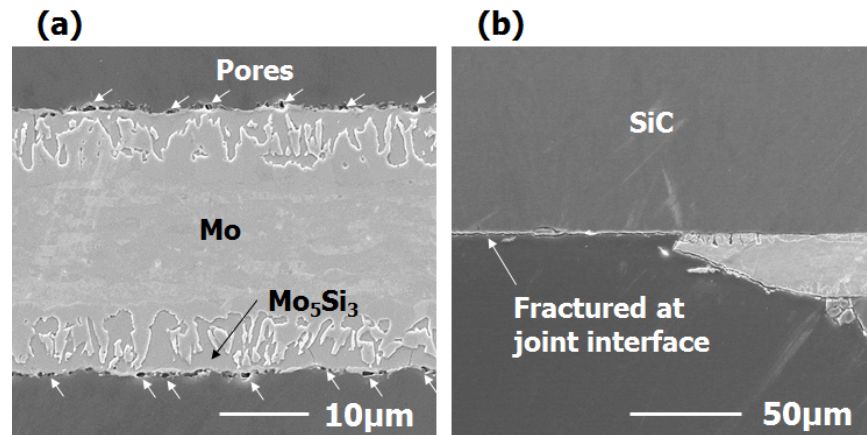


Figure 5. Secondary electron (SE) images of Mo foil joint hot pressed at 1300°C for 1 h: (a) joint interface before DNS test and (b) joint interface after DNS test.

The Mo joints formed at 1500 and 1700 °C with and without oxygen eliminator show similar microstructure to each other as shown in Figure 6. These joint layers mainly consisted of Mo₂C at the center of the joint layer and Mo₅Si₃ sandwiched by Mo₂C and SiC, based on XRD and SEM-EDS analysis. Note that vertical cracks to the joint interface were observed in all the specimens. A phase containing Mo and Si is forming a very thin layer between SiC and Mo₅Si₃, the thickness of which is similar among those joints. This thin layer was also observed and

identified as Mo_5Si_3 by Martinelli using XRD and EDS [4]. A few μm pores located at the joint interface formed at 1500°C using H_2 , despite its highest nominal shear strength. This result indicates that this kind of small pore was not critical flaw for the Mo joint in this work. The similar microstructure with the different strength may be caused by the difference of the quality of the joint layer. The impurities oxygen is one of the causes affecting that. Differential amount and distribution of carbon and/or Mo_5Si_3 phase formed in Mo_5Si_3 phase [4] also potentially affect the mechanical properties of the Mo_5Si_3 phase.

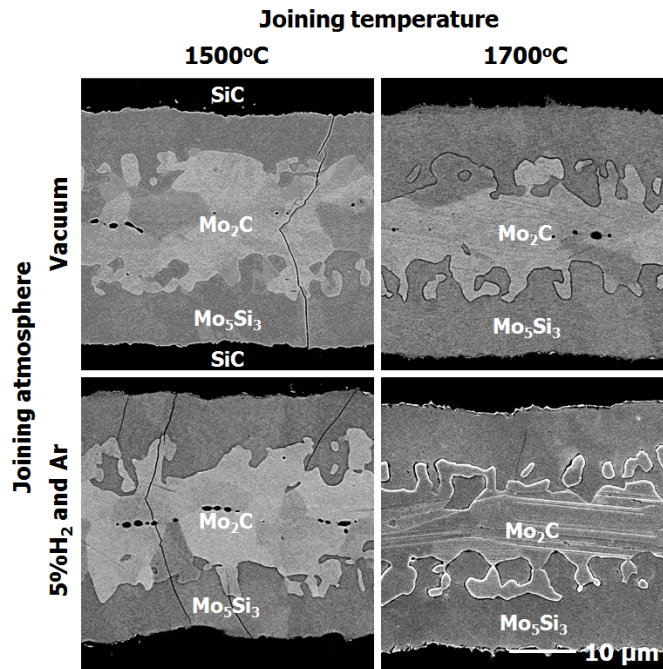


Figure 6. Back scattering electron (BSE) images of the Mo joints formed at 1500 and 1700 °C with and without oxygen eliminator.

2.3.3 MAX-phase pressureless joining

The Hyper-Therm proprietary Ti-Si-C MAX-phase bonding produced the decent joints of CVD SiC with the average shear strength ~ 70 MPa and the coefficient of variation less than 10%.

2.3.4 NITE joining

The microstructure of NITE slurry joint hot pressed at 1860°C for 1 h at 20 MPa is shown in Figure 7. The bonding layer appeared to be inhomogeneous with a substantial spatial variation in the apparent density. The bonding layer achieved a good physical contact with the SiC base only at the dense location. Considerable volume shrinkage due to burning organic binders and sintering during hot pressing may have led to this inhomogeneous microstructure when the slurry

is only insufficiently mixed before being applied to the bonding surfaces. The fracture occurred at the joint/base interface is possibly due to debonding at the porous location. Achieving uniform and dense NITE joint with good contact with the SiC base is the key to guide improving this joining procedure.

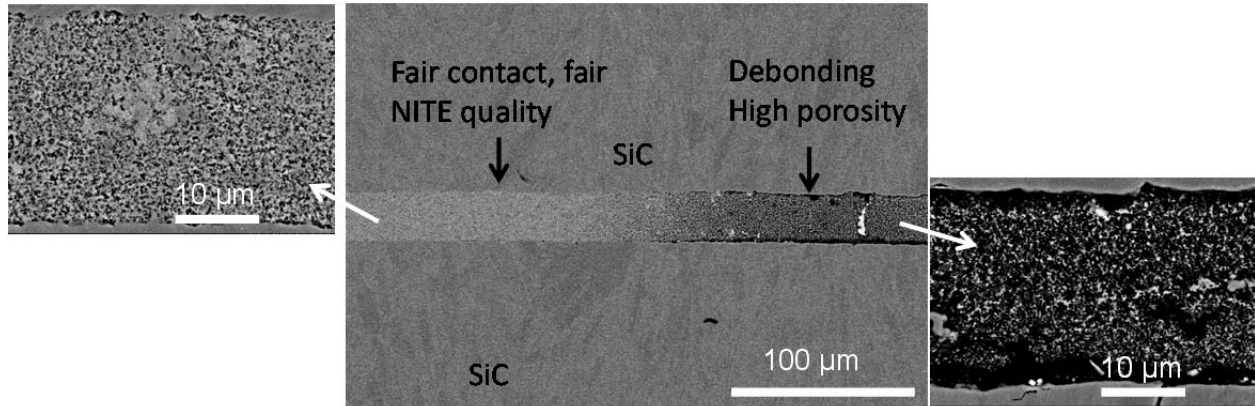


Figure 7. Back scattering electron (BSE) images of NITE slurry joint hot pressed at 1860°C for 1h.

In order to achieve a more uniform and dense NITE joint with good contact with the SiC base, multiple approaches have been implemented, including increasing viscosity of the NITE slurry or the sintering aids concentration, improving the uniformity of the NITE slurry layer by ultrasonic spray coating (USC), screen printing, or grinding CVD SiC to minimize bonding interface unevenness, etc. Figure 8 shows an example of microstructure of the USC NITE slurry joint hot pressed at 1875°C for 1 h at 20 MPa (slight temperature difference from the earlier work shall not lead to significant joint quality evolution). Unlike the NITE joint applied by manually painting onto the bonding surface, the USC NITE joint appears to be much denser, whereas significant pores observed within the joint. However, more porous localized regions were also found, implying limited sintering at some local regions. The fracture occurred at the joint/base interface due to less base contact at the fairly porous joint. The average shear strength of the USC NITE joint increased to 67.3 MPa from 43.9 MPa for the manual painted slurry joints. However, strength of the USC NITE joint is still significantly lower than those reported previously [5]. The large standard deviation of 33.2 MPa indicates that a significant improvement in the spatially uniformity for this joint is achievable.

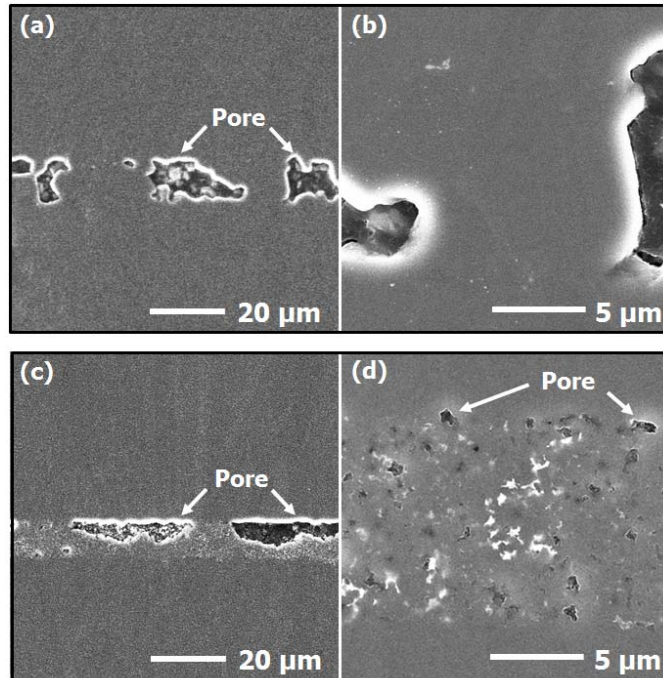


Figure 8. Secondary electron images of ultrasonically spray-coated NITE slurry joint hot pressed at 1875°C for 1 h. (a, b): Well sintered region with large pores; (c, d): more porous region.

3. IRRADIATION PROGRAM

3.1 TEST METRIX AND SCHEDULE

It is planned that a series of rabbit capsules containing the SiC joint specimens are irradiated in the flux trap facility in HFIR. The experiment is designated as HFIR SCJ-2 (the second campaign of silicon carbide joint irradiation). The irradiation conditions and the preliminary specimen matrix are defined below in Table 3 with the schedule and the post-irradiation examination (PIE) plan in Table 4.

In the previous study conducted as a part of the ORNL and international fusion materials research and development program, several variations of silicon carbide joints were neutron-irradiated in HFIR nominally at 500°C and 800°C to the maximum dose of ~5 dpa. The joint materials included the CVD SiC, monolithic and fiber composite materials made through the NITE process, joined by the titanium diffusion bonding, calcia-alumina (CA) glass-ceramic joining, Ti-Si-C MAX phase joining, NITE slurry joining, and NITE green tape joining. The post-irradiation examination for this experiment showed encouraging results including the retention of the pre-irradiation strength after irradiation to 3 to 5 dpa at 500°C and 800°C [ref]. The new SCJ-2 experiment will evaluate the effect of neutron irradiation to higher fluence levels at the LWR-relevant (~300°C) temperature, on SiC joints prepared in this work or by collaborators. The joint materials that are planned or considered to be irradiated in this campaign are listed in Table 5.

Table 3. List of capsules and irradiation conditions. The Round A irradiation is currently scheduled to initiate in early FY-2014. The Round B irradiation is temporarily planned to initiate in FY-2015.

ID	T _{irr} (°C)	Dose ¹	Exp. Round
SCJ2-02	300	8	A
SCJ2-03	300	8	A
SCJ2-04	300	8	B
SCJ2-05	300	8	B
SCJ2-06	300	8	B
SCJ2-07	300	8	B
SCJ2-08	300	8	B
SCJ2-09	300	8	B

1: $\times 10^{25}$ n/m², E>0.1MeV

Table 4. Updated schedule of the irradiation program

Task	Round A	Round B
Capsule design update	FY13	FY13
Capsule parts procurement	FY13	FY13
Specimen delivery	FY14/Q1	FY15/Q1
Capsule construction / approval	FY14/Q1-2	FY15/Q1-2
Irradiation	FY14/Q3-	FY15/Q3-
Capsule shipment / disassembly	FY15/Q3	FY16/Q3
Post-irradiation examination	FY15/Q4-	FY16/Q4-

Table 5. Materials considered for irradiation study

Material description	Supplier
General Atomics Proprietary, Polymer/CVD Hybrid	General Atomics
Rolls-Royce HTC Proprietary, Pressureless MAX-phase	Rolls-Royce HTC
Ti Diffusion Bonding	ORNL
Mo Diffusion Bonding	ORNL
NITE, Slurry*	Kyoto University
NITE, Green Tape*	Kyoto University
Calcia-Alumina Glass-Ceramics*	Politecnico di Torino
MAX-phase, Green Tape*	PNNL ¹
Metallic Braze*	Ceramatec
NITE, spray coating*	ORNL
NITE, screen printing*	ORNL
NITE, Pressureless Sintering*	ORNL

*Final test matrix will be determined based on availability of these samples.

1: Pacific Northwest National Laboratory

3.2 IRRADIATION VEHICLE DEVELOPMENT

The rabbit capsule design to be used will be in principle identical with the one used in the previous campaign. Each capsule contains sixteen (16) joint specimens. The specimen type used will be the miniature torsional hourglass specimen that was previously designed and designated as Type 6SQ-5D, 6SQ-4D, or 6SQ-5V. The capsule design is provided in Appendix A. The drawings of the specimens are provided in Appendix B. The capsules planned are listed in Table 3. The preliminary schedule for the SCJ-2 irradiation campaign supported by the LWRS Program is given in Table 4.

A three-dimensional finite element thermal analysis was performed for the capsules with the initial design attributes for ~300°C. The result is presented in Attachment 3, indicating needs for further design iterations to achieve the temperature distributions within an acceptable range.

4. REFERENCES

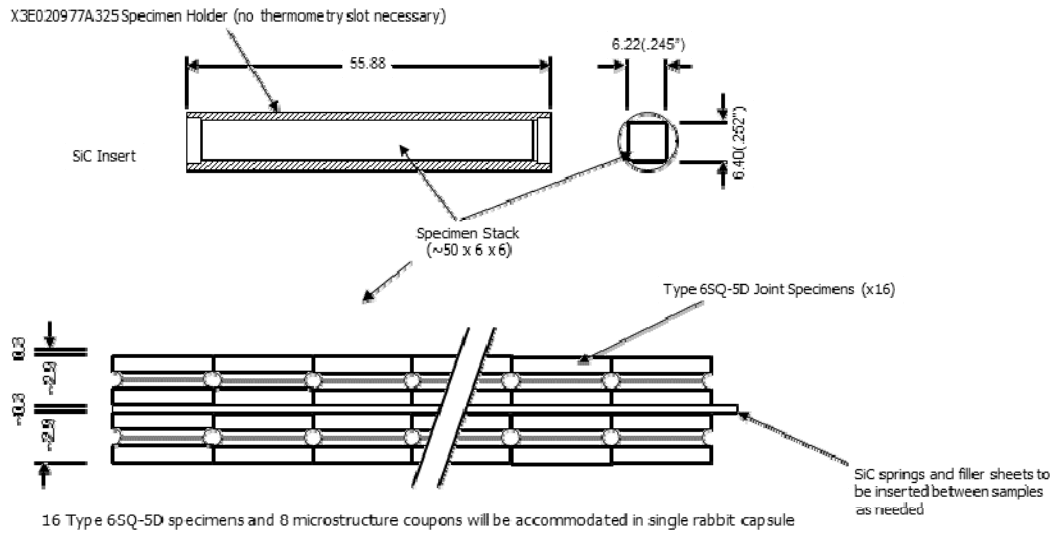
- [1] B. Gottselig, E. Gyarmati, A. Naoumidis, H. Nickel, Joining of ceramics demonstrated by the example of SiC/Ti, *J. Eur. Ceram. Soc.*, 6 (1990) 153-160.
- [2] B.V. Cockeram, The diffusion bonding of silicon carbide and boron carbide using refractory metals, 1999.
- [3] Y. Katoh, T. Cheng, J.O. Kiggans, J.L. McDuffee, L.L. Snead, Status of Irradiation Test Preparation Activities for Silicon Carbide Joining and Irradiation Studies, ORNL/TM-2012/597, in, Oak Ridge National Laboratory, Oak Ridge, 2012.
- [4] A.E. Martinelli, R.A.L. Drew, Microstructural development during diffusion bonding of α -silicon carbide to molybdenum, *Mater. Sci. Eng. A*, 191 (1995) 239-247.
- [5] Y. Katoh, L.L. Snead, C. Shih, T. Hinoki, T. Koyanagi, T. Toyoshima, M. Ferraris, A. Ventrella, C.H. Henagar, Irradiation-Resistant Joining for Silicon Carbide Ceramics and Composites, *J. Nucl. Mater.*, (Submitted).

APPENDIX A: CAPSULE DESIGN DRAWINGS

SIC Torsional Joint Capsule (Rev. 100316)

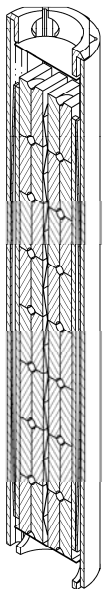
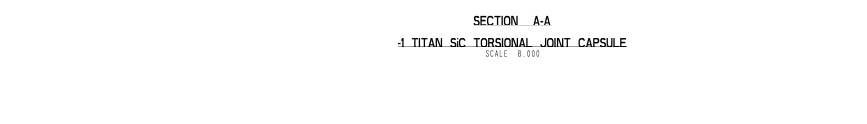
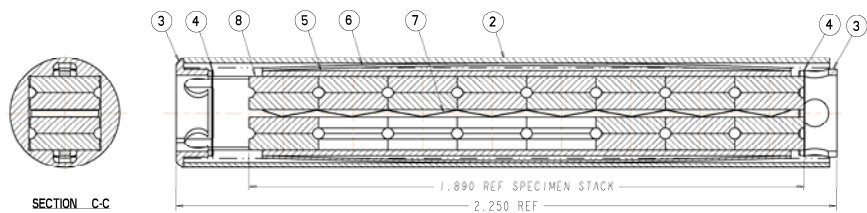
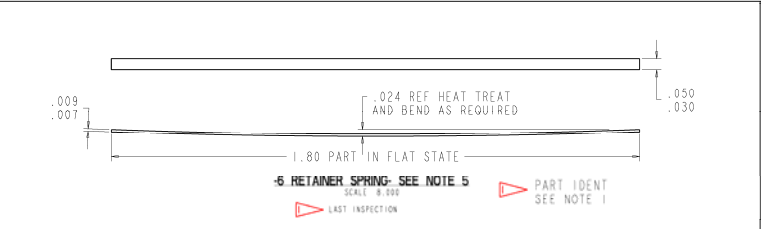
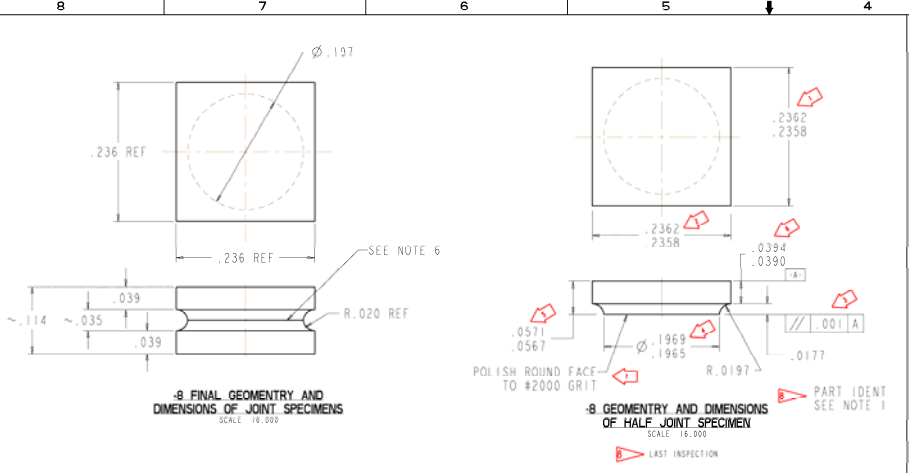
List of internal parts (= inside sleeve) and specimens

Part #	Name	Material	Qty / Capsule
1	Thermometry Bar	CVD SIC HR grade	2
N/A	8 Specimen (Type 6SQ-5D)	SIC (CVD or composite)	16
N/A	8 Specimen (Coupon)	SIC (CVD or composite)	8



Printed 1/4/2006 3:29 PM

Yutal Katoch (376-3996, A-14648006_katoch@ornl.gov)



THIS DWG	CAGE CODE	PART OR IDENTIFYING NO	NUMERATURE OR DESCRIPTION	MATERIAL	FIND NO
16		-8 THIS DWG	TYPE 850-SB JOINT SPECIMEN	SiC (CVD OR COMPOSITE)	8
17		-8 THIS DWG	CENTER SPACER	GRAPHITE	7
1		-6 THIS DWG	RETAINER SPRING	SiC	6
2		#3EG20977AS40-3	SMALL THERMOMETRY	CVD SiC 9H GRADE	5
2		#3EG20977AS40-2	SUPPORT DISK	MC6Y3Si3N6	4
2		#3EG20977AS40-1	CENTERING THIMBLE	VARADUM OR VARADUM ALLOY	3
1		JLMO421202B-1	-1 SPECIMEN HOLDER TYPE A	MC6Y3Si3N6	2
1		-1	TITAN SiC TORSIONAL JOINT CAPSULE		1

NOTE: APPLICABLE SPECIFICATIONS SHOWN ARE OMNI RESEARCH REACTORS DIVISION (ORRD) ENGINEERING SPECIFICATIONS FOR HFIR. SUBSTITUTE NUCLEAR SCIENCE AND TECHNOLOGY DIV. (NSTD) TECH LEADER OR HIS DESIGNEE FOR RDD TASK LEADER.

CERTIFIED FOR CONSTRUCTION
ISSUE DATE:

GENERAL NOTES:

- PART SHALL BE PLACED IN A SEALABLE PLASTIC BAG WITH A TAG INDICATING PART IDENTIFICATION OF THE FORM "DRAWING NO.-PART NO.-SERIAL NO." OR AN INSPECTION REQUEST NO. (I.R.N.) TRACEABLE TO MATERIAL AND PART DOCUMENTATION. ONLY THE LAST FOUR DIGITS OF THE DRAWING NUMBER ARE REQUIRED.
- CLEAN PER AP-NSTD-20977-020.
- DIMENSIONS ARE IN INCHES.
- MATERIAL TO BE SUPPLIED BY CUSTOMER ALONG WITH APPROPRIATE MATERIAL CERTIFICATION DOCUMENTATION.
- SPRING (FIND #6) DIMENSIONS MAY BE MODIFIED TO MEET REQUIREMENTS OF EXPERIMENT.
- JOINT LAYER IS TYPICALLY LESS THAN 50 MICRONS. JOINING AGENT MAY BE (1) SiC, (2) TI-Si-C, OR (3) CA-AL-O.

ALL DIMENSIONS UNLESS OTHERWISE SPECIFIED ARE IN INCHES. TOLERANCES UNLESS OTHERWISE SPECIFIED ARE: DIMENSIONS IN PARENTHESIS (±) ±0.0005; DIMENSIONS IN SQUARES (±) ±0.0005; DIMENSIONS IN CIRCLES (±) ±0.0005; DIMENSIONS IN TRIANGLES (±) ±0.0005; DIMENSIONS IN DIAMETERS (±) ±0.0005; DIMENSIONS IN RADIUSES (±) ±0.0005.

REV	DESCRIPTION	BY	TL	DATE	FR	DATE	LOG	DATE	CHK'D	DATE	APPROV'D	DATE

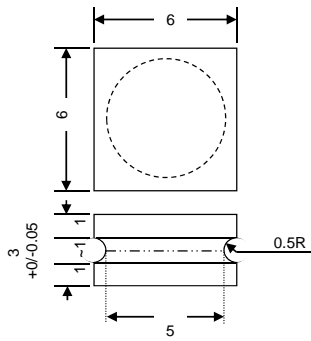
SCALE	DES. J. L. MODIFIED BY DATE

UT-BATTELLE Oak Ridge National Laboratory
HFIR TARGET IRRADIATION CAPSULE
RABBIT CAPSULE
TITAN SiC TORSIONAL JOINT SHEAR TEST

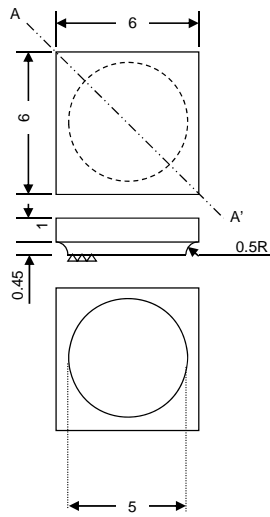
JLMO32320.0

APPENDIX B: SPECIMEN DRAWINGS

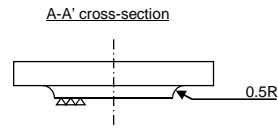
Miniature Joint Specimen for Torsional Shear Test: Type 6SQ-5D (6x6x3 mm)



Final geometry and dimensions of the joint specimen

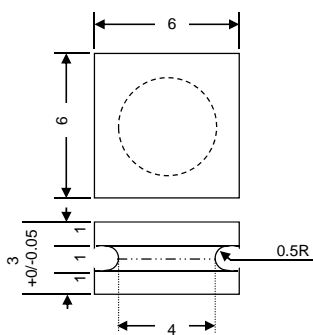


1/2 Joint Specimen

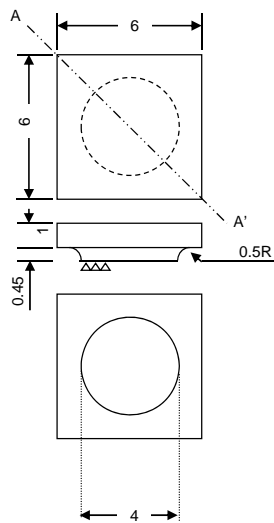


- Notes
1. Units are in millimeter unless otherwise noted.
 2. Specimen is prepared either by machining of final specimen after joining or joining after machining a pair of 1/2 specimens.
 3. Material is standard grade Rohm and Haas CVD SiC.
 4. Tolerance for envelope dimensions is +0/-10 microns.
 5. Two faces (square top face and round bottom face) have to be sufficiently parallel.
 6. The round face needs to be polished to #2000 grit.

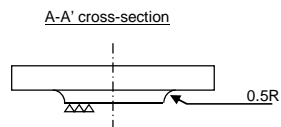
Miniature Joint Specimen for Torsional Shear Test: Type 6SQ-4D (6x6x3 mm)



Final geometry and dimensions of the joint specimen



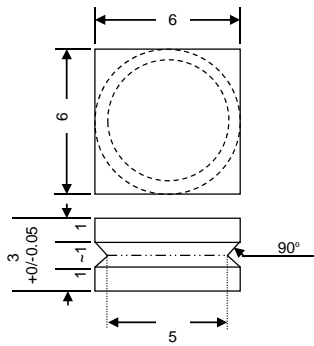
1/2 Joint Specimen



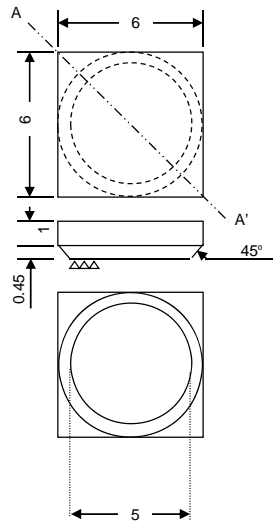
Notes

1. Units are in millimeter unless otherwise noted.
2. Specimen is prepared either by machining of final specimen after joining or joining after machining a pair of 1/2 specimens.
3. Material is standard grade Rohm and Haas CVD SiC.
4. Tolerance for envelope dimensions is +0/-10 microns.
5. Two faces (square top face and round bottom face) have to be sufficiently parallel.
6. The round face needs to be polished to #2000 grit.

Miniature Joint Specimen for Torsional Shear Test: Type 6SQ-5V (6x6x3 mm)

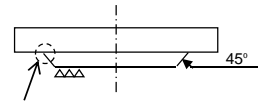


Final geometry and dimensions of the joint specimen



1/2 Joint Specimen

A-A' cross-section

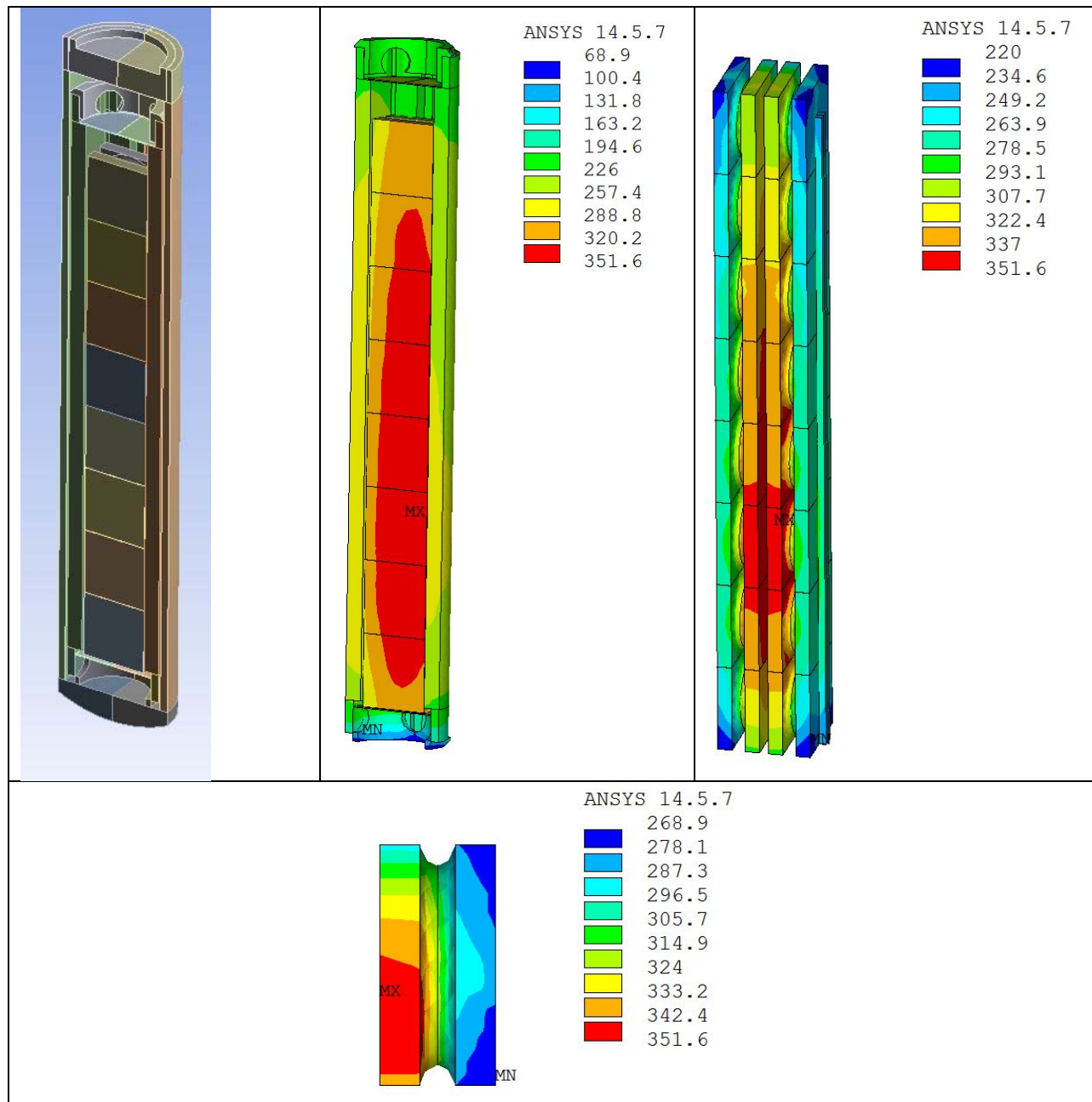


Finite radius ($R \sim 0.5$ mm) is tolerated.

Notes

1. Units are in millimeter unless otherwise noted.
2. Specimen is prepared either by machining of final specimen after joining or joining after machining a pair of 1/2 specimens.
3. Material is standard grade Rohm and Haas CVD SiC.
4. Tolerance for envelope dimensions is +0/-10 microns.
5. Two faces (square top face and round bottom face) have to be sufficiently parallel.
6. The round face needs to be polished to #2000 grit.

APPENDIX C: UPDATED THERMAL ANALYSIS RESULTS



Half-cut three-dimensional model developed for thermal analysis of the SiC torsional joint rabbits (top left), temperature distribution at inside surface of specimens stack (top center), temperature distribution of the entire specimens stack (top right), and temperature distribution within one of the hot specimens (bottom). Despite the relatively large temperature distribution within the specimens stack, the joint planes are maintained in a temperature range 290 – 320 °C for all specimens.

 TEMPERATURE DESIGN SOLUTION FOR SiC JOINT-JOINT RABBITS

 DESCRIPTION

- * 300.°C target temperature
- * Helium fill gas
- * 15.84 cm bottom location

 BOUNDARY CONDITIONS

Heat transfer coefficient = 47700. W/m²•°C
 Bulk coolant temperature = 53.6 °C

 HEAT GENERATION

Part	Material	Heat Gen. @Midplane (W/kg)	----- Heat Load ----- @Midplane (W)	@Location (W)
1) Specimen 1D	SiC(Irr)	31700.	9.3	6.8
2) Specimen 1C	SiC(Irr)	31700.	9.3	6.8
3) Specimen 2D	SiC(Irr)	31700.	9.3	6.7
4) Specimen 2C	SiC(Irr)	31700.	9.3	6.7
5) Specimen 3D	SiC(Irr)	31700.	9.3	6.5
6) Specimen 3C	SiC(Irr)	31700.	9.3	6.5
7) Specimen 4D	SiC(Irr)	31700.	9.3	6.3
8) Specimen 4C	SiC(Irr)	31700.	9.3	6.3
9) Specimen 5D	SiC(Irr)	31700.	9.3	6.2
10) Specimen 5C	SiC(Irr)	31700.	9.3	6.2
11) Specimen 6D	SiC(Irr)	31700.	9.3	6.0
12) Specimen 6C	SiC(Irr)	31700.	9.3	6.0
13) Specimen 7D	SiC(Irr)	31700.	9.3	5.9
14) Specimen 7C	SiC(Irr)	31700.	9.3	5.9
15) Specimen 8D	SiC(Irr)	31700.	9.3	5.7
16) Specimen 8C	SiC(Irr)	31700.	9.3	5.7
17) Housing	AL-6061	31300.	57.4	38.5
18) Housing	AL-6061	31300.	57.4	38.5
19) Housing upper	AL-6061	31300.	2.6	1.5
20) Housing upper	AL-6061	31300.	2.6	1.5
21) Housing lower	AL-6061	31300.	7.6	5.7
23) Housing lower	AL-6061	31300.	7.6	5.7
25) Housing end cap	AL-6061	31300.	8.2	4.8
26) Housing end cap	AL-6061	31300.	8.2	4.8
27) Holder	V-4Cr4Ti	45900.	160.1	107.7
29) Holder	V-4Cr4Ti	45900.	160.3	107.8
30) Holder upper	V-4Cr4Ti	45900.	6.0	3.6
31) Holder upper	V-4Cr4Ti	45900.	6.0	3.6
33) Holder lower	V-4Cr4Ti	45900.	6.3	4.7

34) Holder lower	V-4Cr4Ti	45900.	6.3	4.7
36) Cent.Thimble (lower)	Ti-6Al4V	35200.	2.2	1.7
37) Cent.Thimble (lower)	Ti-6Al4V	35200.	2.2	1.7
38) Disk lower	Ti-6Al4V	35200.	0.3	0.2
39) Disk lower	Ti-6Al4V	35200.	0.3	0.2
40) Thermometry	SiC(Irr)	31700.	2.2	1.5
41) Thermometry	SiC(Irr)	31700.	2.2	1.5
42) Spring thermometry	SiC(Irr)	31700.	0.9	0.6
43) Spring thermometry	SiC(Irr)	31700.	0.9	0.6
44) Disk upper	Ti-6Al4V	35200.	0.3	0.2
45) Disk upper	Ti-6Al4V	35200.	0.3	0.2
46) Cent.Thimble (upper)	Ti-6Al4V	35200.	2.2	1.3
47) Cent.Thimble (upper)	Ti-6Al4V	35200.	2.2	1.3
-----			660.7	444.1

CAPSULE TEMPERATURE SUMMARY

Name	Material	Tavg	Tmin	Tmax	T.025	T.975

1) Specimen 1D	SiC(Irr)	261.	220.	309.	231.	282.
2) Specimen 1C	SiC(Irr)	311.	242.	338.	269.	333.
3) Specimen 2D	SiC(Irr)	284.	258.	322.	269.	299.
4) Specimen 2C	SiC(Irr)	333.	279.	349.	297.	348.
5) Specimen 3D	SiC(Irr)	287.	269.	325.	276.	301.
6) Specimen 3C	SiC(Irr)	337.	291.	352.	301.	350.
7) Specimen 4D	SiC(Irr)	285.	265.	321.	274.	299.
8) Specimen 4C	SiC(Irr)	334.	287.	349.	299.	348.
9) Specimen 5D	SiC(Irr)	281.	261.	318.	269.	295.
10) Specimen 5C	SiC(Irr)	329.	282.	344.	294.	342.
11) Specimen 6D	SiC(Irr)	276.	255.	311.	264.	290.
12) Specimen 6C	SiC(Irr)	322.	276.	338.	288.	335.
13) Specimen 7D	SiC(Irr)	268.	245.	304.	255.	282.
14) Specimen 7C	SiC(Irr)	313.	265.	330.	280.	327.
15) Specimen 8D	SiC(Irr)	254.	221.	292.	234.	270.
16) Specimen 8C	SiC(Irr)	300.	241.	318.	265.	315.
17) Housing	AL-6061	58.	56.	62.	56.	60.
18) Housing	AL-6061	58.	55.	62.	56.	59.
19) Housing upper	AL-6061	56.	56.	57.	56.	56.
20) Housing upper	AL-6061	56.	55.	56.	56.	56.
21) Housing lower	AL-6061	65.	60.	67.	61.	67.
23) Housing lower	AL-6061	65.	60.	68.	61.	67.
25) Housing end cap	AL-6061	70.	68.	71.	69.	71.
26) Housing end cap	AL-6061	71.	70.	72.	70.	71.
27) Holder	V-4Cr4Ti	262.	196.	289.	218.	285.
29) Holder	V-4Cr4Ti	250.	196.	276.	214.	269.
30) Holder upper	V-4Cr4Ti	208.	191.	222.	195.	218.
31) Holder upper	V-4Cr4Ti	205.	191.	215.	195.	212.
33) Holder lower	V-4Cr4Ti	195.	151.	233.	166.	221.
34) Holder lower	V-4Cr4Ti	192.	156.	221.	167.	214.
36) Cent.Thimble (lower)	Ti-6Al4V	147.	69.	228.	89.	209.

37) Cent.Thimble (lower)	Ti-6Al4V	146.	73.	227.	90.	208.
38) Disk lower	Ti-6Al4V	259.	211.	308.	219.	304.
39) Disk lower	Ti-6Al4V	266.	211.	310.	220.	309.
40) Thermometry	SiC(Irr)	267.	237.	282.	242.	278.
41) Thermometry	SiC(Irr)	267.	237.	282.	242.	278.
42) Spring thermometry	SiC(Irr)	257.	221.	270.	232.	268.
43) Spring thermometry	SiC(Irr)	257.	221.	270.	232.	268.
44) Disk upper	Ti-6Al4V	233.	207.	246.	216.	245.
45) Disk upper	Ti-6Al4V	230.	206.	246.	214.	244.
46) Cent.Thimble (upper)	Ti-6Al4V	211.	163.	219.	199.	218.
47) Cent.Thimble (upper)	Ti-6Al4V	209.	163.	214.	198.	214.
ALL SPECIMENS	SiC(Irr)	298.	220.	352.	249.	347.

PROPERTY SUMMARY AT THE AVERAGE PART TEMPERATURE

Name	Material	Thermal Cond. (W/m•°C)	Thermal Exp. Coeff. (µm/m•°C)	Emis (---)
1) Specimen 1D	SiC(Irr)	6.651	3.14	0.900
2) Specimen 1C	SiC(Irr)	6.627	3.30	0.900
3) Specimen 2D	SiC(Irr)	6.640	3.22	0.900
4) Specimen 2C	SiC(Irr)	6.618	3.36	0.900
5) Specimen 3D	SiC(Irr)	6.639	3.23	0.900
6) Specimen 3C	SiC(Irr)	6.616	3.37	0.900
7) Specimen 4D	SiC(Irr)	6.640	3.22	0.900
8) Specimen 4C	SiC(Irr)	6.617	3.36	0.900
9) Specimen 5D	SiC(Irr)	6.641	3.21	0.900
10) Specimen 5C	SiC(Irr)	6.619	3.35	0.900
11) Specimen 6D	SiC(Irr)	6.644	3.19	0.900
12) Specimen 6C	SiC(Irr)	6.623	3.33	0.900
13) Specimen 7D	SiC(Irr)	6.648	3.16	0.900
14) Specimen 7C	SiC(Irr)	6.627	3.31	0.900
15) Specimen 8D	SiC(Irr)	6.654	3.12	0.900
16) Specimen 8C	SiC(Irr)	6.633	3.27	0.900
17) Housing	AL-6061	166.480	24.21	0.050
18) Housing	AL-6061	166.452	24.21	0.050
19) Housing upper	AL-6061	166.177	24.21	0.050
20) Housing upper	AL-6061	166.163	24.21	0.050
21) Housing lower	AL-6061	167.223	24.21	0.050
23) Housing lower	AL-6061	167.248	24.21	0.050
25) Housing end cap	AL-6061	167.897	24.21	0.050
26) Housing end cap	AL-6061	167.949	24.21	0.050
27) Holder	V-4Cr4Ti	32.582	9.71	0.350
29) Holder	V-4Cr4Ti	32.449	9.69	0.350
30) Holder upper	V-4Cr4Ti	32.029	9.65	0.350
31) Holder upper	V-4Cr4Ti	31.998	9.65	0.350
33) Holder lower	V-4Cr4Ti	31.910	9.64	0.350
34) Holder lower	V-4Cr4Ti	31.886	9.63	0.350

36) Cent.Thimble (lower)	Ti-6Al4V	9.467	9.65	0.320
37) Cent.Thimble (lower)	Ti-6Al4V	9.452	9.65	0.320
38) Disk lower	Ti-6Al4V	11.787	9.81	0.334
39) Disk lower	Ti-6Al4V	11.899	9.82	0.338
40) Thermometry	SiC(Irr)	6.648	3.16	0.900
41) Thermometry	SiC(Irr)	6.648	3.16	0.900
42) Spring thermometry	SiC(Irr)	6.652	3.13	0.900
43) Spring thermometry	SiC(Irr)	6.653	3.13	0.900
44) Disk upper	Ti-6Al4V	11.205	9.75	0.320
45) Disk upper	Ti-6Al4V	11.143	9.75	0.320
46) Cent.Thimble (upper)	Ti-6Al4V	10.734	9.70	0.320
47) Cent.Thimble (upper)	Ti-6Al4V	10.680	9.69	0.320

 RADIAL DIMENSIONS AND GAP SUMMARY FOR THE HOLDER-HOUSING GAP

	Minimum	Maximum	Average
Contact status	1.0	1.0	1.0
Contact temperature (°C)	122.	211.	185.
Target temperature (°C)	57.	60.	59.
Gap (µm)	174.340	183.622	177.309
Contact pressure (MPa)	0.000	0.000	0.000
Conductance coefficient (W/m ² •°C)	982.	1130.	1081.
Total heat flux (kW/m ²)	101.65	249.97	203.15
Gap conductance heat flux (kW/m ²)	101.59	249.72	203.01
Radiation heat flux (kW/m ²)	0.06	0.23	0.17
Contact conduction heat flux (kW/m ²)	0.00	0.00	0.00